

Article

Effect of Mo Content on Microstructure and Property of Low-Carbon Bainitic Steels

Haijiang Hu, Guang Xu *, Mingxing Zhou and Qing Yuan

The State Key Laboratory of Refractories and Metallurgy, Key Laboratory for Ferrous Metallurgy and Resources Utilization of Ministry of Education, Wuhan University of Science and Technology, Wuhan 430081, China; hhjsunny@sina.com (H.H.); kdmingxing@163.com (M.Z.); 15994235997@163.com (Q.Y.)

* Correspondence: xuguang@wust.edu.cn; Tel.: +86-27-6886-2813

Academic Editor: Soran Biroscu

Received: 17 June 2016; Accepted: 19 July 2016; Published: 23 July 2016

Abstract: In this work, three low-carbon bainitic steels, with different Mo contents, were designed to investigate the effects of Mo addition on microstructure and mechanical properties. Two-step cooling, i.e., initial accelerated cooling and subsequent slow cooling, was used to obtain the desired bainite microstructure. The results show that the product of strength and elongation first increases and then shows no significant change with increasing Mo. Compared with Mo-free steel, bainite in the Mo-containing steel tends to have a lath-like morphology due to a decrease in the bainitic transformation temperature. More martensite transformation occurs with the increasing Mo, resulting in greater hardness of the steel. Both the strength and elongation of the steel can be enhanced by Mo addition; however, the elongation may decrease with a further increase in Mo. From a practical viewpoint, the content of Mo could be ~0.14 wt. % for the composition design of low-carbon bainitic steels in the present work. To be noted, an optimal scheme may need to consider other situations such as the role of sheet thickness, toughness behavior and so on, which could require changes in the chemistry. Nevertheless, these results provide a reference for the composition design and processing method of low-carbon bainitic steels.

Keywords: bainitic transformation; low carbon; microstructure; property

1. Introduction

Low-carbon bainitic steels are used widely in many industrial fields due to their favorable combination of strength and toughness. For the composition design of low-carbon bainitic steels, several alloying elements such as B, Mo, and Cr are usually added to achieve sufficient hardenability [1–4]. In doing so, the desired microstructure of bainitic ferrite is obtained during continuous cooling in industrial production processes.

Since B-Mo bainitic steel was developed by Pickering and Irvine [5], the function of Mo in steels has been widely investigated by many researchers. It is generally accepted that Mo addition can separate the bainitic transformation zone to obtain the desired bainitic microstructure over a wide range of cooling rates [6,7]. Mo is added to decrease the diffusion coefficient of carbon, resulting in the retardation of ferrite and pearlite transformation. Khare et al. [8] stated that the most dramatic effect of Mo is to hinder high temperature transformation, but 0.25 wt. % Mo had no significant influence on bainitic transformation kinetics in a 0.32 wt. % C bainite steel. Sourmail et al. [9] reported that the effect of Mo on bainite transformation was not clear with negligible or no retardation influence on the bainite formation kinetics, although the calculated effect on the driving force led to an expected acceleration. However, Kong et al. [10] claimed that bainitic transformation in a low-carbon alloyed steel containing 0.40 wt. % Mo was slowed down when the cooling rate was below 15 °C/s. Chen et al. [11] reported that it is necessary to add suitable Mo to improve the toughness and strength of high Nb-bearing

X80 pipeline steels (0.26 wt. % Mo, 0.07 wt. % Nb). They considered that Mo addition can suppress pearlite and ferrite (PF) transformation and decrease the transformation temperature, resulting in refined transformed products, so the mechanical properties are improved.

Although the effects of Mo on transformation, microstructure and properties of low-carbon bainitic steels have been widely investigated by several studies, an optimal scheme on the amount of Mo to be added is not fully understood. In most works, the amount of Mo added to low-carbon bainitic steels is designed to be ≥ 0.25 wt. % [12–16], which could be considered an expensive addition in the modern context. It is necessary to optimize the amount of Mo added for commercial scenarios. So far, how the comprehensive mechanical properties, especially the product of strength and elongation (PSE), change with the amount of Mo added has seldom been investigated.

Therefore, in the present work, three low-carbon bainitic steels were designed to investigate the effect of Mo content on the PSE. The evolution of the bainitic microstructure with Mo addition was also analyzed. The results provide a theoretical reference for the composition design of low-carbon bainitic steels.

2. Materials and Methods

Three low-carbon bainitic steels with the chemical compositions given in Table 1 were refined using a 100 kg vacuum furnace. Steel #1 was free from Mo and acted as a standard with which the Mo-bearing steels could be compared. The cast ingots were heated to 1250 °C before hot-rolling to 12-mm-thick plates by seven passes. The starting temperatures of the rough roll and finishing roll processes were 1070 °C and 880 °C, respectively. After hot rolling, the plates were initially fast cooled to 500 °C at ~ 30 °C/s, then air cooled to room temperature. This experimental procedure is basically consistent with the industrial technology. The bainite starting temperature (B_s) and martensite starting temperature (M_s) of three tested steels were calculated according to the following equations [17]:

$$B_s = 839 - \sum_i P_i x_i - 270 \times [1 - \exp(-1.33x_c)] \quad (1)$$

$$M_s = 565 - \sum_i K_i x_i - 600 \times [1 - \exp(-0.96x_c)] \quad (2)$$

where $i = \text{Mn, Si, Cr, Ni, and Mo}$, and the concentration x in wt. %.

$$\sum_i P_i x_i = 86x_{\text{Mn}} + 23x_{\text{Si}} + 67x_{\text{Cr}} + 67x_{\text{Ni}} + 75x_{\text{Mo}} \quad (3)$$

$$\sum_i K_i x_i = 31x_{\text{Mn}} + 13x_{\text{Si}} + 10x_{\text{Cr}} + 18x_{\text{Ni}} + 12x_{\text{Mo}} \quad (4)$$

Table 1. Chemical compositions of steels (wt. %).

Steel	C	Si	Mn	Mo	P	S	B_s	M_s
#1	0.223	1.523	2.187	0	<0.01	<0.003	546	357
#2	0.219	1.504	2.095	0.134	<0.01	<0.003	543	360
#3	0.225	1.519	2.034	0.273	<0.01	<0.003	538	358

The aim of calculating B_s and M_s is to design the finishing temperature point of the fast cooling stage and the results are given in Table 1. The specimens were mechanically polished and etched with a 4% nital solution for microstructure examination using optical microscopy (OM) and scanning electron microscopy (SEM). The morphology of bainitic ferrite was examined using a Nova 400 Nano field emission scanning electron microscope (FEI, Hillsboro, OR, USA) operated at an accelerating voltage of 20 kV. In addition, the fine microstructure was observed using a JEM-2100F transmission electron

microscope (TEM, JEOL, Tokyo, Japan). The volume fractions of retained austenite (RA) in different samples were determined using an X'Pert diffractometer (Panalytical, Almelo, The Netherlands) with Co K α radiation under the following conditions: acceleration voltage, 40 kV; current, 150 mA; and step, 0.06°. Tensile tests were performed using a UTM-5305 electronic universal tensile machine (Instron, Norwood, MA, USA) at room temperature. Tensile specimens were prepared according to ASTM standards and the strain rate was $\sim 4 \times 10^{-3}$ /s. Vickers hardness tests were performed with a HV1000A micro-hardness tester (0.2 kg-1960 mN, Matsuzawa, Tokyo, Japan). The average value of at least ten individual measurements was calculated, including several martensite bands and bainite blocks in the microstructure.

3. Results and Discussions

3.1. Characteristics of Microstructure

Optical micrographs of the specimens are presented in Figure 1. It can be seen that bainite was obtained in all samples with or without Mo addition. In steel #1 (Figure 1a), the microstructure mainly consists of bainite with a very small amount of martensite/austenite (M/A) islands. The microstructure is fine due to the initial fast cooling rate of ~ 30 °C/s. Martensite in bands (darker regions in Figure 1b,c) appears in Mo-added steels. Actually, microstructural bands are caused by the segregation of the substitutional alloying element of manganese, which is abundant in these materials. Compared to steel #1, the microstructure of steels #2 and #3 is finer.

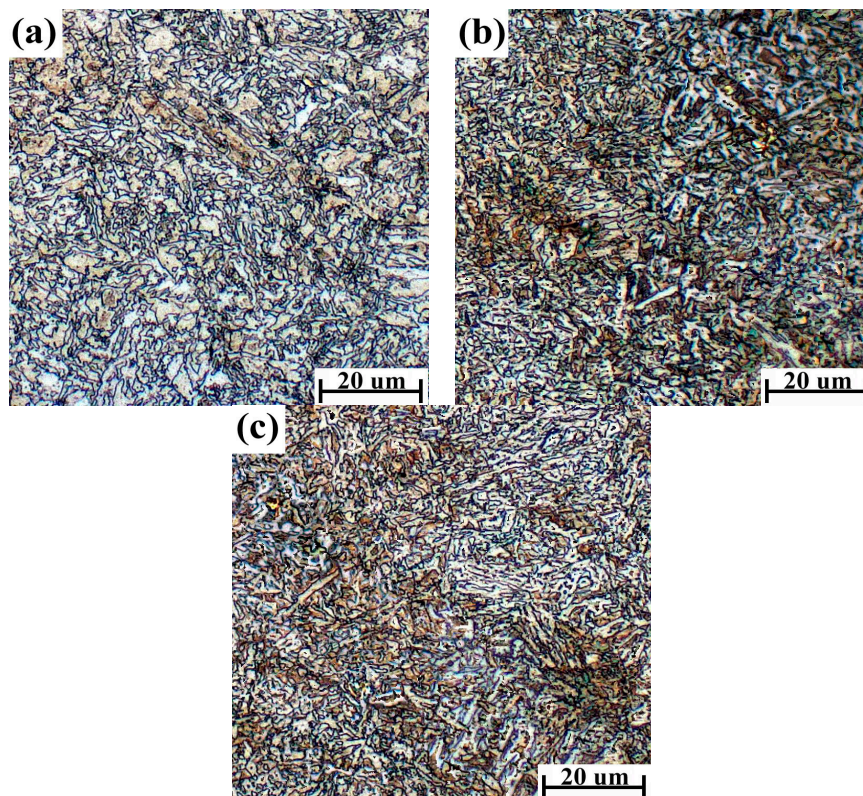


Figure 1. Optical micrographs of steels with different Mo content: (a) steel #1, Mo-free; (b) steel #2, 0.134 wt. % Mo; (c) steel #3, 0.273 wt. % Mo.

In order to further clarify the changes in the microstructure, SEM micrographs of steels with different Mo additions are given in Figure 2. The microstructure in the Mo-free steel consists of granular bainite (GB) and M/A islands, shown by the arrow in Figure 2a. With a 0.134 wt. % Mo addition, lath bainite (LB), GB and M/A islands are observed (Figure 2b); the amount of GB decreases

and the M/A islands become finer. From Figure 2c, it can be seen that the amount of LB increases with increasing Mo. The results indicate that Mo can decrease the amount of GB transformed by undercooled austenite, and contributes to obtaining LB and fine M/A islands during the continuous cooling process.

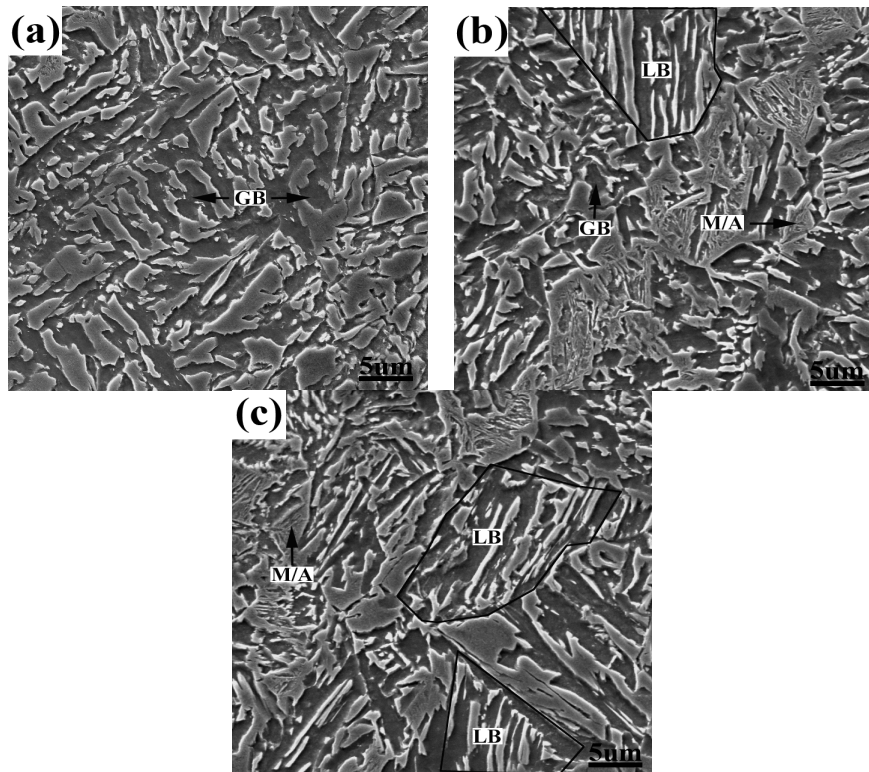


Figure 2. SEM micrographs of steels with different Mo contents: (a) steel #1, Mo-free; (b) steel #2, 0.134 wt. % Mo; (c) steel #3, 0.273 wt. % Mo.

The appearance of LB and M/A islands demonstrates that bainite transformation in Mo-containing steel occurs at a lower temperature range than in Mo-free steel. As the strong carbide-forming element Mo is added to the steel, the carbon diffusion activation energy in austenite increases and the carbon diffusion coefficient decreases [10]. Bainite transformation is closely related to carbon diffusion. Therefore, bainite transformation starts at a lower temperature range when Mo is added. As the B_s point decreases, the parent austenite transforms into LB at a low transformation temperature. In addition, a phenomenon called “incomplete transformation” usually occurs because bainite transformation stops prematurely before the equilibrium amount is attained [18,19]. Thus, residual austenite after bainite transformation partially transforms to martensite.

Figure 3 shows TEM micrographs of the microstructure of the three tested steels. The morphologies of GB and LB are clearly presented, as shown in Figure 3a–c. The bainite in steel #1 (Mo-free) is almost GB with little LB, whereas the microstructure in steel #2 (0.134 wt. % Mo) consists of GB and LB (Figure 3b). With the increase of Mo, the amount of LB increases and the width of the bainitic laths decreases (Figure 3c). In addition, net-like dislocation lines are observed on the surface of LB, as shown in Figure 3d. When adding Mo to steel, the morphology of bainite changes from GB to LB and dislocation begins to occur. This is due to the decrease of the transformation temperature, which changes the mechanism of bainite transformation. The relatively high dislocation density associated with bainitic ferrite is often attributed to the shape deformation caused by displacive transformation [20]. Caballero et al. [21] investigated the influence of the transformation temperature on the dislocation density and the corresponding bainitic ferrite thickness. They found that the

dislocation density increased with a decrease in the transformation temperature and the corresponding bainitic ferrite thickness decreased.

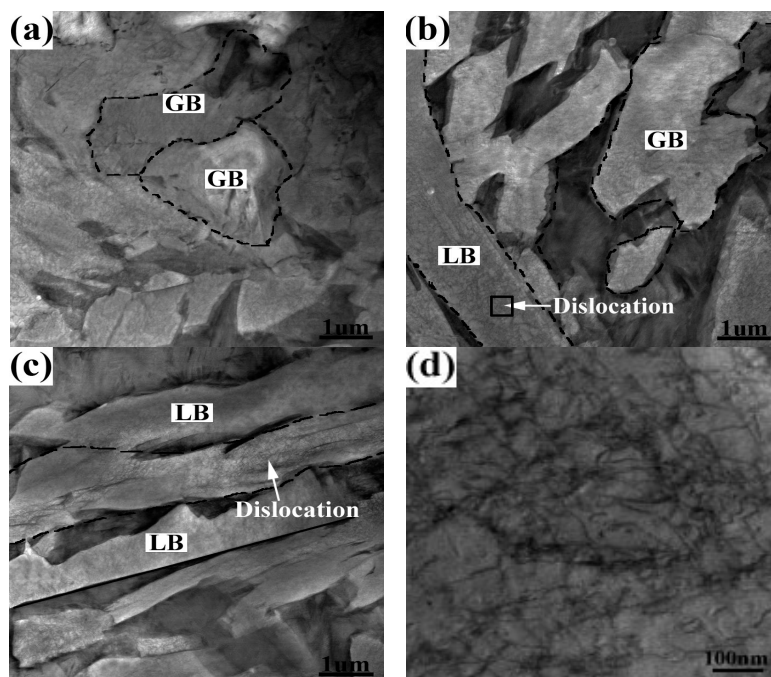


Figure 3. TEM micrographs showing the morphology of bainite and dislocation: (a) steel #1, Mo-free; (b) steel #2, 0.134 wt. % Mo; (c) steel #3, 0.273 wt. % Mo; (d) micrograph in high magnification of the square zone in (b).

3.2. Quantitative Analysis

The calculation of RA is based on integrated intensities of the $(200)_\alpha$, $(211)_\alpha$, $(200)_\gamma$, $(220)_\gamma$ and $(311)_\gamma$ diffraction peaks obtained by X-ray diffraction (XRD). The volume fractions of RA were calculated according to Equation (5) and the value is the average of V_i [22].

$$V_i = \frac{1}{1 + G(I_\alpha/I_\gamma)} \quad (5)$$

where V_i is the volume fraction of austenite for each peak, I_α and I_γ are the integrated intensities of ferrite and austenite peaks, respectively, and G is a certain value for each peak. As bainite and martensite have a similar crystalline structure, it is difficult to distinguish them in the diffraction diagrams. The volume fraction of bainite was evaluated using the method in Reference [23]. The results of the quantitative analysis are given in Table 2. In order to minimize error, an average value of each case was obtained from at least 10 individual measurements. The volume fraction of GB decreased with Mo content, whereas the volume fractions of LB and M increased. The Mo-containing steels had more RA than the Mo-free steel, demonstrating that Mo addition contributes to the stabilization of austenite.

Table 2. Quantitative data on the microstructure of different steels.

Sample	V_{GB}	V_{LB}	V_M	V_γ
#1 (Mo-free)	0.69 ± 0.04	0.05 ± 0.01	0.19 ± 0.02	0.07 ± 0.01
#2 (0.134% Mo)	0.39 ± 0.03	0.25 ± 0.02	0.25 ± 0.03	0.11 ± 0.01
#3 (0.273% Mo)	0.06 ± 0.01	0.47 ± 0.03	0.37 ± 0.03	0.10 ± 0.01

Notes: V_{GB} , volume fraction of granular bainite; V_{LB} , volume fraction of lath bainite; V_M , volume fraction of martensite; V_γ volume fraction of RA (determined by electron micrographs and XRD).

3.3. Mechanical Properties

The tensile test results of the three steels are given in Table 3. The results are the average values of four tests. The yield strength (YS) and ultimate tensile strength (UTS) are improved by the addition of Mo. Meanwhile, the total elongation (TE) first increases and then decreases within a small range. The percentage reduction of area (Z) also changes a little with varying Mo content. As mentioned previously, the addition of Mo decreases the transformation temperature of bainite, resulting in a finer bainitic microstructure and a certain amount of martensite. Moreover, LB provides a higher phase strengthening effect than GB. These two reasons lead to the increase in strength of the Mo-containing steel compared to the Mo-free steel. It should be noted that the increment of UTS (112 MPa, Mo from 0 to 0.134 wt. %; 56 MPa, Mo from 0.134 wt. % to 0.273 wt. %) reduces with the increment of the Mo content. For the industrial production of low-carbon bainitic steels, comprehensive mechanical properties are normally considered. Thus, the value of PSE, i.e., $UTS \times TE$ (GPa %), versus Mo addition is plotted in Figure 4. It can be observed that the PSE showed no significant change when the Mo content went beyond 0.134 wt. %. This is due to the slow increase in strength and decrease in elongation. In many current studies, the amount of Mo added to low-carbon bainitic steels is normally designed to be ≥ 0.25 wt. % [12–16]. However, in the present study, it is demonstrated that it is more suitable to add Mo at ~ 0.134 wt. % considering the production cost. It should be noted that an optimal scheme sometime needs to consider other factors such as the role of sheet thickness, toughness behavior and so on which could require changes in the chemistry. Nevertheless, the result of the present work provides a reference for the composition and processing design of low-carbon bainitic steels.

Table 3. Mechanical properties of samples with different compositions.

Steel	YS (MPa)	UTS (MPa)	TE (%)	Z (%)	PSE (GPa %)
#1	561	1015	15.6	41	15.8
#2	583	1127	18.3	37	20.6
#3	610	1173	16.8	38	19.7

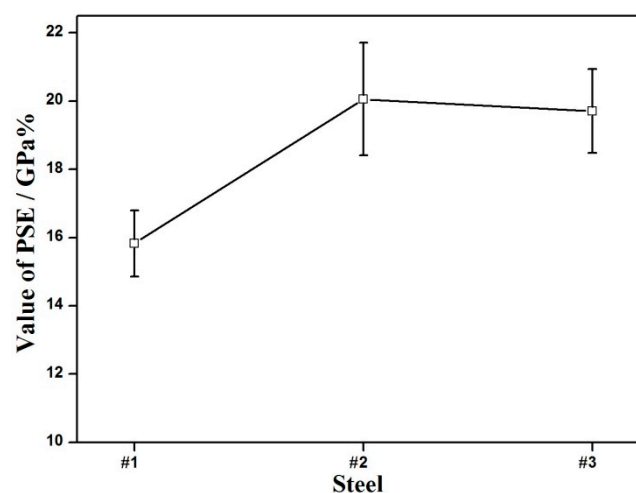


Figure 4. The product of strength and elongation (PSE) in steels with different Mo contents.

Figure 5 shows the results of the Vickers micro-hardness tests. The average value of the micro-hardness in steel #1 (4.83 GPa) is the lowest of all the steels. The highest hardness values of steels #2 and #3 reach ~ 5.5 GPa, which corresponds to the M/A constituents in the microstructure. In addition, the ratio of the high hardness value in steel #3 is larger than that in steel #2, which is due to the larger amount of martensite. Moreover, the bainite matrix is harder in the Mo-containing steel

than in the Mo-free one. The occurrence of LB contributes to the increase of the hardness of the matrix. The results of the hardness tests are closely related to the microstructure (Figures 1 and 2).

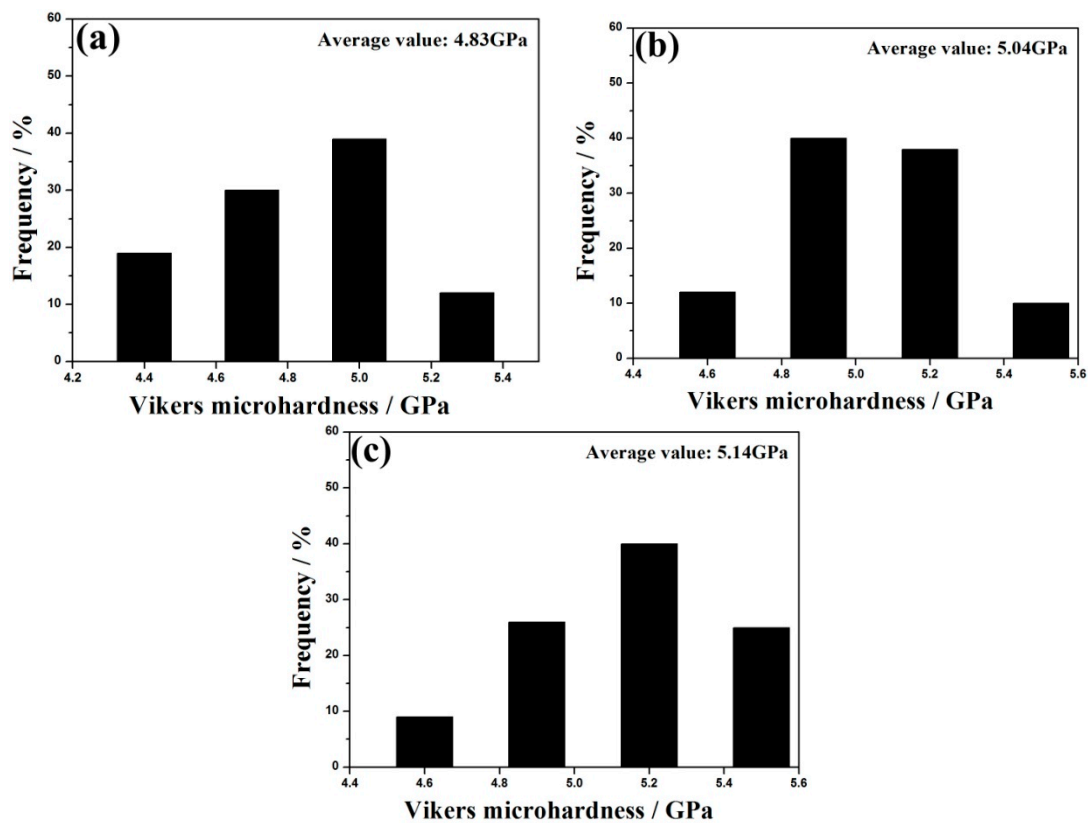


Figure 5. Vickers micro-hardness values of samples with different Mo content: (a) steel #1, Mo-free (b) steel #2, 0.134 wt. % Mo, (c) steel #3, 0.273 wt. % Mo.

3.4. Design of Processing

As discussed above, the constitution and morphology of the microstructure are changed by adding Mo into steels. It is inferred that the transformation kinetics are affected by the addition of Mo. Time-temperature-transformation (TTT) diagrams are often used as references for the design of the composition and processing technology of low-carbon bainitic steels [24,25]. Figure 6 shows the TTT diagrams calculated based on the compositions of tested steels by MUCG83 [26,27]. Compared to the Mo-free steel, both steels #2 and #3 have an obvious bay between the two C-curves (one at high temperature representing reconstructive transformation and the other at low temperature representing displacive transformation [27]). This is due to Mo enhancing the hardenability of the steel, causing a separation of the bainite C-curve. In addition, when the Mo content is increased from 0.134 wt. % to 0.273 wt. %, the C-curves show no significant change. Kong et al. [9] reported that 0.40 wt. % Mo can further reduce the Bs when the cooling rate is low, but the difference is not obvious when the cooling rate is above 30 °C/s. The calculated TTT diagrams suggest that a two-step cooling regime is a promising method for producing an optimal bainite microstructure. The results in the present work provide a practical reference for the design of the composition and processing routes of low-carbon bainitic steels.

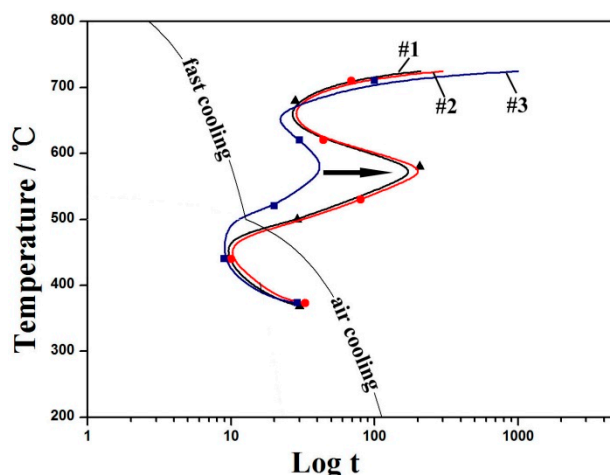


Figure 6. Calculated TTT diagrams for the Mo-free steel (#1) and the Mo-containing steels (#2 and #3).

4. Conclusions

Three low-carbon bainitic steels were designed to investigate the effects of Mo addition on the microstructure and mechanical properties. The results show that the microstructure in Mo-free steel consists of GB + M/A with little LB, whereas the microstructure in Mo-added steels consists of GB + LB + M/A. With increasing the Mo, the amount of LB increases and the bainite laths become finer. The product of strength and elongation first increases and then shows no significant change with further Mo addition. Lath-like bainite and M/A islands in the Mo-bearing steels contribute to the increase in strength and the improvement in elongation compared to the Mo-free steel. However, the elongation may decrease with increasing Mo. From a practical viewpoint, the content of Mo could be ~0.14 wt. % for the composition design of low-carbon bainitic steels in the present work. It should be noted that an optimal scheme sometime needs to consider other factors such as the role of sheet thickness, toughness behavior and so on which could require changes in the chemistry. Nevertheless, the result of the present work provides a reference for the composition and processing design of low-carbon bainitic steels.

Acknowledgments: The authors are grateful for the financial supports from the National Natural Science Foundation of China (NSFC) (No. 51274154), the State Key Laboratory of Development and Application Technology of Automotive Steels (Baosteel Group) (No. 20121101).

Author Contributions: Guang Xu and Haijiang Hu conceived and designed the experiments; Haijiang Hu performed the experiments; Haijiang Hu and Mingxing Zhou analyzed the data; Qing Yuan contributed materials and tools; Haijiang Hu wrote the paper.

Conflicts of Interest: The authors declare no conflict of interest. The founding sponsors had no role in the design of the study; in the collection, analyses, or interpretation of data; in the writing of the manuscript, and in the decision to publish the results.

Abbreviations

The following abbreviations are used in this manuscript:

PSE	product of strength and elongation
LSCM	high temperature laser scanning confocal microscopy
B _s	bainite starting temperature
M _s	martensite starting temperature
OM	optical microscopy
SEM	scanning electron microscopy
TEM	transmission electron microscope
XRD	X-ray diffractogram
M/A	martensite/austenite
GB	granular bainite

LB	lath bainite
RA	retained austenite
YS	yield strength
UTS	ultimate tensile strength
TE	total elongation
TTT	time-temperature-transformation

References

1. Soliman, M.; Palkowski, H. Development of the low temperature bainite. *Arch. Civ. Mech. Eng.* **2016**, *16*, 403–412. [[CrossRef](#)]
2. Furuhashi, T.; Tsuzumi, K.; Miyamoto, G.; Amino, T.; Shigesato, G. Characterization of Transformation Stasis in Low-Carbon Steels Microalloyed with B and Mo. *Metall. Mater. Trans. A* **2014**, *45A*, 5990–5996. [[CrossRef](#)]
3. Bhadeshia, H.K.D.H. Computational design of advanced steels. *Scr. Mater.* **2014**, *70*, 12–17. [[CrossRef](#)]
4. Hu, Z.W.; Xu, G.; Yang, H.L.; Zhang, C.; Yu, R. The Effects of Cooling Mode on Precipitation and Mechanical Properties of a Ti-Nb Microalloyed Steel. *J. Mater. Eng. Perform.* **2014**, *23*, 4216–4222. [[CrossRef](#)]
5. Ivine, K.J.; Pickering, F.B. Low Carbon Bainitic Steels. *J. Iron Steel Inst.* **1957**, *187*, 292–309.
6. Grange, R.A. Estimating the hardenability of carbon steels. *Metall. Trans. B* **1973**, *4*, 2231–2244. [[CrossRef](#)]
7. Pickering, F.B. *Physical Metallurgy and the Design of Steels*; Applied Science Publishers Ltd.: London, UK, 1978.
8. Khare, S.; Lee, K.; Bhadeshia, H.K.D.H. Relative effects of Mo and B on ferrite and bainite kinetics in strong steels. *Int. J. Mater. Res.* **2009**, *100*, 1513–1520. [[CrossRef](#)]
9. Sourmail, T.; Smanio, V. Low temperature kinetics of bainite formation in high carbon steels. *Acta Mater.* **2013**, *61*, 2639–2648. [[CrossRef](#)]
10. Kong, J.H.; Xie, C.S. Effect of molybdenum on continuous cooling bainite transformation of low-carbon microalloyed steel. *Mater. Des.* **2006**, *27*, 1169–1173. [[CrossRef](#)]
11. Chen, X.W.; Qiao, G.Y.; Han, X.L.; Wang, X.; Xiao, F.R.; Liao, B. Effects of Mo, Cr, and Nb on microstructure and mechanical properties of heat affected zone for Nb-bearing X80 pipeline steels. *Mater. Des.* **2014**, *53*, 888–901. [[CrossRef](#)]
12. Soliman, M.; Mostafa, H.; El-Sabbagh, A.S.; Palkowski, H. Low temperature bainite in steel with 0.26 wt. % C. *Mater. Sci. Eng. A* **2010**, *527*, 7706–7713. [[CrossRef](#)]
13. Qian, L.; Zhou, Q.; Zhang, F.; Meng, J.; Zhang, M.; Tian, Y. Microstructure and mechanical properties of a low carbon carbide-free bainitic steel co-alloyed with Al and Si. *Mater. Des.* **2012**, *39*, 264–268. [[CrossRef](#)]
14. Wang, Y.H.; Zhang, F.C.; Wang, T.S. A novel bainitic steel comparable to maraging steel in mechanical properties. *Scr. Mater.* **2013**, *68*, 763–766. [[CrossRef](#)]
15. Long, X.Y.; Zhang, F.C.; Kang, J.; Lv, B.; Shi, X.B. Low-temperature bainite in low-carbon steel. *Mater. Sci. Eng. A* **2014**, *594*, 344–351. [[CrossRef](#)]
16. Wang, X.L.; Wu, K.M.; Hu, F.; Yu, L.; Wan, X.L. Multi-step isothermal bainitic transformation in medium-carbon steel. *Scr. Mater.* **2014**, *74*, 56–59. [[CrossRef](#)]
17. Bohemen, S.M.C. Bainite and martensite start temperature calculated with exponential carbon dependence. *Mater. Sci. Technol.* **2012**, *28*, 487–495. [[CrossRef](#)]
18. Aaronson, H.I.; Reynolds, W.T.; Purdy, G.R. The incomplete transformation phenomenon in steel. *Metall. Mater. Trans. A* **2006**, *37A*, 1731–1745. [[CrossRef](#)]
19. Xia, Y.; Miyamoto, G.; Yang, Z.G.; Zhang, C.; Furuhashi, T. Direct measurement of carbon enrichment in the incomplete bainite transformation in Mo added low carbon steels. *Acta Mater.* **2015**, *91*, 10–18. [[CrossRef](#)]
20. Bhadeshia, H.K.D.H.; Christian, J.W. Bainite in steels. *Metall. Trans.* **1990**, *21A*, 767–769. [[CrossRef](#)]
21. Caballero, F.G.; Garcia-Mateo, C.; Santofimia, M.J.; Miller, M.K.; de Andrés, C.G. New experimental evidence on the incomplete transformation phenomenon in steel. *Acta Mater.* **2009**, *57*, 8–17. [[CrossRef](#)]
22. Wang, C.Y.; Shi, J.; Cao, W.Q.; Dong, H. Characterization of microstructure obtained by quenching and partitioning process in low alloy martensitic steel. *Mater. Sci. Eng. A* **2010**, *527*, 3442–3449. [[CrossRef](#)]
23. Hu, H.J.; Xu, G.; Wang, L.; Xue, Z.L.; Zhang, Y.L.; Liu, G.H. The Effects of Nb and Mo Addition on Transformation and Properties in Low Carbon Bainitic Steels. *Mater. Des.* **2015**, *84*, 95–99. [[CrossRef](#)]
24. Caballero, F.G.; Santofimia, M.J.; Capdevila, C.; Garcia-Mateo, C.; de Andrés, C.G. Design of advanced bainitic steels by optimization of TTT diagrams and T₀ curves. *ISIJ Int.* **2006**, *46*, 1479–1488. [[CrossRef](#)]

25. Caballero, F.G.; Santofimia, M.J.; García-Mateo, C.; Chao, J.; de Andrés, C.G. Theoretical design and advanced microstructure in super high strength steels. *Mater. Des.* **2009**, *30*, 2077–2083. [[CrossRef](#)]
26. Bhadeshia, H.K.D.H. A thermodynamic analysis of isothermal transformation diagrams. *Met. Sci.* **1982**, *16*, 159–165. [[CrossRef](#)]
27. Bhadeshia, H.K.D.H. *Bainite in Steels*; Institute of Materials: London, UK, 1992; pp. 1–450.



© 2016 by the authors; licensee MDPI, Basel, Switzerland. This article is an open access article distributed under the terms and conditions of the Creative Commons Attribution (CC-BY) license (<http://creativecommons.org/licenses/by/4.0/>).